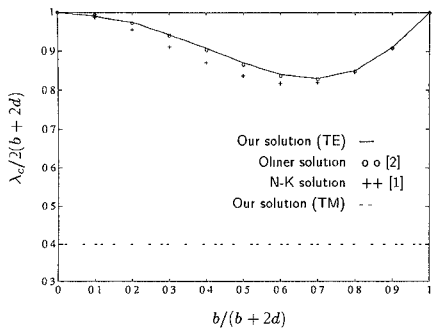

Fig. 2. Theoretical values of $\lambda_c/2(b+2d)$ versus relative width $b/(b+2d)$ of groove, where λ_c is the cutoff wavelength and $a/(b+2d) = 0.2$.

mode approximate solutions are obtained in low-frequency limit and are shown to be accurate for most practical applications.

REFERENCES

[1] T. Nakahara and N. Kurauchi, "Transmission modes in the grooved guide," *J. Inst. Electron. Commun. Eng. Jap.*, vol. 47, no. 7, pp. 43–51, July 1964.

[2] A. A. Oliner and P. Lampariello, "The dominant mode properties of open groove guide: An improved solution," *IEEE Trans. Microwave Theory Tech.*, vol. MTT-33, pp. 755–764, Sept. 1985.

[3] Inderjit and M. Sachidananda, "Rigorous analysis of a groove guide," *IEE Proc.-H*, vol. 139, no. 5, pp. 449–452, Oct. 1992.

[4] M. Zhewang, Y. Eikichi, and X. Shanjia, "Modal analysis of open groove guide with arbitrary groove profile," *IEEE Microwave and Guided Wave Lett.*, vol. 2, no. 9, pp. 364–366, Sept. 1992.

[5] T. J. Park, H. J. Eom, and K. Yoshitomi, "An analysis of transverse electric scattering from a rectangular channel in a conducting plane," *Radio Sci.*, vol. 28, no. 5, pp. 663–673, Sept.–Oct. 1993.

Phasor Diagram Analysis of Millimeter-Wave HEMT Mixers

Youngwoo Kwon and Dimitris Pavlidis

***Abstract*—A phasor diagram method is developed based on an analytic approach for conversion gain evaluation in HEMT mixers. The analytical expressions derived in this work take into account the mixing terms of nonlinear elements and provide a simple method to evaluate the conversion gain. The phasor diagram analysis offers physical insight into the mixing mechanisms and identifies the role of each harmonic of the nonlinear elements of HEMT's on the conversion gain. The method is validated with the experimental data of W-band monolithic InP-based HEMT mixers.**

I. INTRODUCTION

HEMT's are promising nonlinear devices for mixers due to their highly nonlinear transconductance characteristics, as well as their conversion gain capability. Recently, HEMT mixers have been realized up to 94 GHz using InAlAs/InGaAs heterostructures [1], [2]. However, the complicated nature of their equivalent circuits and highly nonlinear characteristics make their analysis and optimization difficult. General mixer design and analysis methods were presented in [3] and [4]. HEMT mixer design is usually based on harmonic balance techniques available nowadays in commercial software packages such as Libra of EEsof. The design procedure involves, in this case, consideration of the HEMT equivalent circuit, and definition of the input and output terminations. Based on these, one can evaluate parameters such as the conversion gain at the intermediate frequencies under various input power levels. Furthermore, it is necessary to understand the role of each nonlinear element and its higher order intermixing terms on the conversion gain in HEMT mixers. In this paper, an analytical expression for the conversion gain is derived using a simplified equivalent circuit model. A phasor diagram analysis is presented, showing the mixing components from each nonlinear element and its higher harmonics. This allows one to obtain physical insight into the mixing mechanisms and provides a simple analytical expression for evaluating and optimizing conversion gain.

Manuscript received September 16, 1994; revised May 25, 1995. This work was supported by URI Contract DAAL 03-92-G-0109.

Y. Kwon was with the Department of Electrical Engineering and Computer Science, University of Michigan, Ann Arbor, MI. He is now with Rockwell Science Center, Thousand Oaks, CA 91360 USA.

D. Pavlidis is with the Department of Electrical Engineering and Computer Science, University of Michigan, Ann Arbor, MI 48109-2122 USA.

IEEE Log Number 9413422.

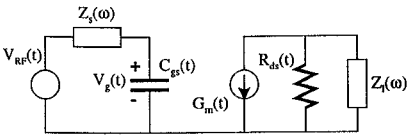

Fig. 1. Simplified equivalent circuit of HEMT mixers used in the phasor diagram analysis.

II. SIMPLIFIED HEMT MIXER THEORY

First, the nonlinearities of the HEMT's are investigated using a combination of a single-tone Harmonic Balance and FFT techniques. The circuit configuration for the calculation was based on the simplified equivalent circuit model of HEMT mixers shown in Fig. 1. Three elements are considered to be nonlinear and participate in the mixing mechanism: C_{gs}, G_m, and R_{ds}. The other elements are taken to be linear and included in the $Z_s(\omega)$ and $Z_l(\omega)$ impedances. The harmonic generation of these three nonlinear elements are investigated as a function of LO power. For this purpose, the device was pumped with a single-tone variable-power LO signal and the time-dependent data of the intrinsic nonlinear parameters were calculated. These time-domain data were then transformed to the frequency-domain data using FFT. Among the three elements, G_m showed the largest harmonic generation. Fig. 2 describes the frequency domain data of G_m as a function of LO power for a 0.1 μm-long, 90 μm-wide gate HEMT using InAlAs/InGaAs heterojunction [5]. The generation of the first harmonic component of G_m (G_{m_1}) is significant at high LO power levels and decreases after a certain power level due to "parasitic MESFET" operation, as shown in [2]. This component is later shown to be most responsible for the mixing mechanism.

Based on the above considerations, an analytical expression is derived for the conversion gain according to the following assumptions and termination conditions:

1) The gate port is short-circuited at the "IF" frequency and only the "Image" and "RF" frequencies are allowed. The higher order harmonics are assumed to be negligibly small, a condition which is satisfied, provided that a proper termination is present

at the gate. Similarly, the drain port is short-circuited at the "RF," "LO" and higher harmonics.

2) For the simplicity of the calculations, the order of R_{ds} nonlinearity is limited to the first harmonics

The derivation basically consists of two parts: one concerning C_{gs} and the other concerning G_m and R_{ds}. The first step is to find out the voltage $V_g(t)$ across C_{gs} as a function of $V_{RF}(t)$ which is the RF excitation voltage. The voltage vector $V_g(t)$ can be expressed as the sum of the voltage phasors as follows

$$V_g(t) = \sum_{n=-\infty}^{\infty} v_{g_n} e^{j(\omega_{RF}+n\omega_{LO})t} \tag{1}$$

where ω_{RF} and ω_{LO} are the RF and LO frequencies; the IF frequency is defined as $\omega_{IF} \equiv \omega_{RF} - \omega_{LO}$. The following voltage relation can then be established between $V_{RF}(t)$ and $V_g(t)$

$$V_g(t) = V_{RF}(t) - Z_s(\omega) \cdot \frac{d}{dt}[C_{gs}(t) \cdot V_g(t)]. \tag{2}$$

A simple expression for $V_g(t)$ can be obtained after straight-forward but rather tedious algebraic manipulations

$$V_g(t) = v_{g_0} e^{j\omega_{RF}t} + v_{g_2}^* e^{j\omega_{IM}t} \tag{3}$$

where ω_{IM} is the image angular frequency, and

$$v_{g_0} = \frac{1 + j\omega_{IM} Z_s(\omega_{IM}) C_{gs_0} \cdot v_{RF}}{\eta} \tag{4}$$

$$v_{g_2}^* = \frac{-j\omega_{IM} Z_s(\omega_{IM}) C_{gs_2} \cdot v_{RF}}{\eta} \tag{5}$$

$$\eta \equiv 1 + jC_{gs_0}[\omega_{RF} Z_s(\omega_{RF}) + \omega_{IM} Z_s(\omega_{IM})] - \omega_{RF}\omega_{IM} Z_s(\omega_{RF}) Z_s(\omega_{IM})(|C_{gs_0}|^2 + |C_{gs_2}|^2) \tag{6}$$

where v_{RF} is the Fourier coefficient of the input RF signal. As shown in the above equations, the second harmonic component of $C_{gs}(t)$ is responsible for the generation of the image frequency component across the input nodes. The image component can eventually be downconverted to the IF frequency by intermixing with other nonlinear components such as G_m and R_{ds}.

The second part of the derivation identifies the mixing terms due to G_m and R_{ds} and evaluates the IF voltage component at the load $[V_{load}(t)]$ as a function of $V_{RF}(t)$. The load voltage, $V_{load}(t)$ can be expressed as a function of $V_g(t)$ as follows

$$V_{load}(t) = -G_m(t) \cdot \frac{R_{ds}(t) \cdot Z_l(\omega)}{R_{ds}(t) + Z_l(\omega)} \cdot V_g(t). \tag{7}$$

After the Fourier expansions of G_m(t) and $R_{ds}(t)$ are introduced to (7) and appropriate rearrangements are made, the following expressions can be obtained

$$V_{load}(t) = -\sum_{l=-N}^{N} g_{m_l} e^{jl\omega_{LO}t} \left\{ Z_l(\omega) - \frac{Z_l^2(\omega)}{Z_l(\omega) + R_{ds_0}} \cdot \sum_{n=-\infty}^{\infty} (-1)^n \mathcal{F}_n(\alpha) e^{jn\omega_{LO}t} \right\} \cdot V_g(t) \tag{8}$$

where $\alpha \equiv R_{ds_1}/(Z_l(\omega) + R_{ds_0})$,

$$\mathcal{F}_n(z) \equiv \sum_{k=0}^{\infty} \binom{2k+n}{k} z^{2k+n} \quad \text{for} \quad n \geq 0$$

and

$$\mathcal{F}_{-n}(z) = \mathcal{F}_n^*(z) \quad \text{for} \quad n < 0 \tag{9}$$

where $\binom{2k+n}{k}$ represents the combinations of $2k+n$ taken k at a time. The complex series function $\mathcal{F}_n(z)$ is here defined for a complex number z and an integer n which identifies the order of the function so that all subsequent equations are expressed with the help of polynomials only. The magnitude of $\mathcal{F}_n(z)$ increases sharply with $|z|$ and drops rapidly with the order n, implying that higher order terms are negligible.

The IF component of the complete HEMT mixer circuit can then be expressed as follows after collecting the $\omega_{RF} - \omega_{LO}$ frequency terms

$$V_{IF}(t) = (v_{g_0} \cdot \psi + v_{g_2}^* \cdot \psi^*) e^{j\omega_{IF}t} \tag{10}$$

where

$$\psi = -g_{m_1}^* \cdot \frac{Z_l(\omega_{IF}) R_{ds_0}}{Z_l(\omega_{IF}) + R_{ds_0}} - \frac{Z_l(\omega_{IF})^2}{Z_l(\omega_{IF}) + R_{ds_0}} \left\{ g_{m_0} \mathcal{F}_1^*(\alpha) + g_{m_1}^*[1 - \mathcal{F}_0(\alpha)] - g_{m_1} \mathcal{F}_2^*(\alpha) - \sum_{l=-N,\, |l|\geq 2}^{N} g_{m_l}(-1)^{l+1} \mathcal{F}_{l+1}^*(\alpha) \right\}.$$

The conversion gain of the mixer can finally be expressed analytically as a function of the harmonics of each nonlinear element by introducing (4) and (5) into (10)

$$\text{Conversion Gain} = \left| \frac{[1 + j\omega_{IM} Z_s(\omega_{IM}) C_{gs_0}] \cdot \psi - j\omega_{IM} Z_s(\omega_{IM}) C_{gs_2} \cdot \psi^*}{\eta} \right|. \tag{11}$$

Here, the first component is the mixing term from the RF frequency at the input which is downconverted to IF through the G_m and R_{ds} harmonics. The second term indicates the downconverted term from the image (IM) frequency through the C_{gs}, G_m, and R_{ds} harmonics. Equation (11) can be plotted in phasor form [Re(conv. gain) versus Im(conv. gain)] and allows one to see the contribution of each nonlinear circuit element (G_m, C_{gs}, and R_{ds}) to the conversion gain.

III. Typical HEMT Mixer Performance Predictions and Comparison with Experiment

To illustrate the applicability of the phasor diagram approach, we considered the HEMT equivalent circuit of Fig. 1 as applied to the InAlAs/InGaAs HEMT for which the nonlinearities are shown in Fig. 2. The source $[Z_s(\omega)]$ and load $[Z_l(\omega)]$ terminations were assumed to be about 10 Ω at 94 GHz and 50 Ω at 3 GHz, respectively. This corresponded to the conditions used for the 94 GHz MMIC HEMT mixer presented in [2]. The mixing terms of (11) can be expressed with the help of phasors in the 2-D complex plane of conversion gain as shown in Fig. 3 for an LO power level of 5 dBm. Each of the vectors indicates the mixing terms from the harmonics of the three nonlinear elements. The following observations can be made from Fig. 3:

1) The major contribution to the conversion gain arises from the g_{m_1} mixing term.

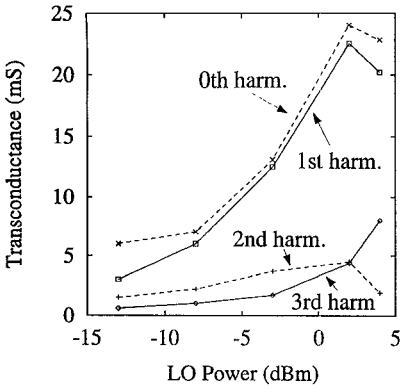

Fig. 2. Harmonic content of G_m as a function of LO power for a 0.1 μm $\times 90\,\mu$m InAlAs/InGaAs HEMT.

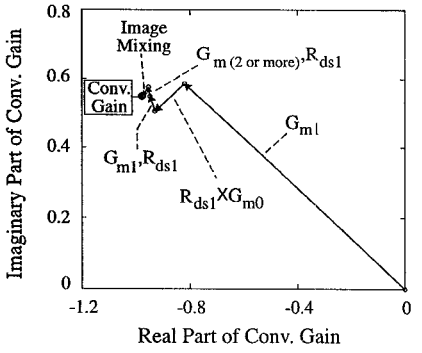

Fig. 3. Phasor diagram of conversion gain vector, showing the various mixing components (P_{LO} = 5 dBm).

2) The r_{ds_1} mixing term multiplied by g_{m_0} degrades the conversion gain due to its incoherent phase with the g_{m_1} mixing term.
3) The intermixing term from g_{m_1} and r_{ds_1} is not negligible and adds in phase to the g_{m_1} term.
4) The contribution from the intermixing terms greater than 2nd order is very small.
5) The image component mixing term is small compared to RF component because of the low c_{gs_2}/c_{gs_0} ratio.
6) Large g_{m_1}/g_{m_0} and r_{ds_0}/r_{ds_1} ratios are needed to obtain optimum conversion gain.

Simulations using various LO power levels showed that the trends described in points in 1–6 apply to a wide range of LO power cases. The results discussed above identify clearly the role of each HEMT parameters on mixer conversion gain and suggest methods of improving the conversion gain through the control of device parameters. Finally, in order to validate the formula, the conversion gain calculated from (11) is compared in Fig. 4 with the measured performance of the 94 GHz monolithic InAlAs/InGaAs HEMT mixers realized by the authors [2]. Also shown is a two-tone harmonic balance simulation obtained for the same device using EEsof-Libra for the same source and load terminations. The complete HEMT equivalent circuit was used for this simulation. Good agreement, within 1 dB, can be seen over a wide range of LO drive levels. The analytic expressions presented in this paper can clearly be used successfully for first pass design and performance estimation of HEMT mixers.

IV. Conclusion

In conclusion, an analytical expression has been derived and a phasor diagram analysis method has been developed which permits an improved physical understanding of the mixing mechanisms and provides a simple method for first pass design of HEMT mixers. Very good agreement was shown between the analytical predictions and the measured performance of monolithic integrated InP-based HEMT mixers operating at 94 GHz.

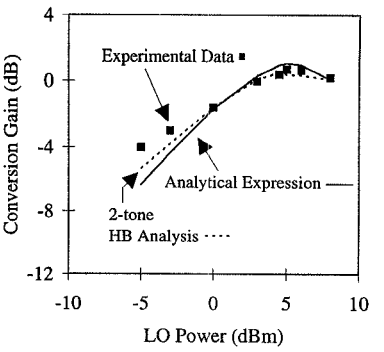

Fig. 4. Comparison of conversion gain calculated using the analytical phasor diagram approach with experimental and 2-tone harmonic balance simulation results for a 94 GHz monolithic InP-based HEMT mixer [2] $V_{gs} = -1.0$ V, $V_{ds} = 1.0$ V.

References

[1] P. D. Chow, K. Tan, D. Streit, D. Garske, P. Liu, and H. C. Yen, "Ultra low noise high gain W-band InP-based HEMT downconverter," in *1991 IEEE Int. Microwave Symp. Dig.*, June 1991, pp. 1041–1044.
[2] Y. Kwon, D. Pavlidis, P. Marsh, G. I. Ng, and T. Brock, "Experimental characteristics and performance analysis of monolithic InP-based HEMT mixers at W-band," *IEEE Trans. Microwave Theory Tech.*, vol. 41, pp. 1–8, Jan. 1993.
[3] D. N. Held and A. R. Kerr, "Conversion loss and noise of microwave and millimeter-wave mixers: Part 1—Theory," *IEEE Trans. Microwave Theory Tech.*, vol. MTT-26, pp. 49–55, Feb. 1978.
[4] S. A. Maas, *Microwave Mixers*. Boston: Artech, 1986.
[5] Y. Kwon, D. Pavlidis, T. Brock, G. I. Ng, K. L. Tan, J. R. Velebir, and D. C. Streit, "Submicron pseudomorphic double heterojunction InAlAs/$In_{0.7}Ga_{0.3}As$/InAlAs HEMT's with high cut-off and current-drive capability," in *Proc. 5th Conf. on InP and Rel. Materials*, Apr. 1993, pp. 465–468.